SPLINE MOJETTE TRANSFORM. APPLICATIONS IN TOMOGRAPHY AND COMMUNICATIONS.

Jean-Pierre Guédon, Nicolas Normand
IRCCyN-IVC CNRS UMR 9567, Ecole polytechnique Université de Nantes, France
Rue Christian Pauc, La chantrerie, BP 60601, Nantes, F44036, France
{jean-pierre.guedon ;nicolas.normand}@polytech.univ-nantes.fr

ABSTRACT The Mojette transform is a fast and exact discrete Radon transform. Its inverse also share the same order of complexity properties. Spline functional spaces are here used to derive a class of new Mojette transforms. Algorithms with linear complexity (in terms of projections and pixels number) are derived. The transform capabilities are shown first to model the discrete tomographic acquisition process. This efficient transform is also exemplified in the area of real-time packet network transmissions where it is able to fight against losses and noise degradations.

1. INTRODUCTION

During the last decade the Shannon's information theory has been generalized by Unser and AlDroubi [1,2,3]. The continuous-discrete equivalence of signals of Shannon's theorem has been extended from the subspace of bandlimited functions to spline subspaces of any order. In this view, the band-limited signals only represents a specific case of a spline subspace of infinite order. This theory is of major practical use when one want to model a specific device or acquired signals. This is particularly true for image acquisition. Section 2 gives some brief recalls on this theory. In section 3, the Dirac-Mojette transform, which is a discrete exact Radon transform, is presented. Some of its application developped for five years are presented. In contrast, section 4 use the spline theory to derive the behavior of the novel spline Mojette transform and explains the design of the exact digital filtering needed for increasing or decreasing the spline order. Section 5 shows two different uses for the obtained class of transform. The first example is image processing and the relationships between the presented operator and classical filtered backprojection (FBP) encountered in tomography. The second example is multimedia transmissions where information packets describing spline Mojette projections are used to fight against noise as a forward error correcting (FEC) scheme.

2. SPLINE INFORMATION THEORY

In this section the results of Unser-AlDroubi theory useful in this paper are briefly recalled. A polynomial spline is a function that is piecewise polynomial of degree n with the additional smoothness constraint that the polynomial segments are connected together in a way that insures the continuity of the function and its derivatives up to order (n-1). In the present context, the generic function space of polynomial splines of order n is denoted by $S_n(IR)$. Specifically, S_n (IR) is the sub-set of functions in $L_2(IR)$ that are of class C_{n-1} and are equal to a polynomial of degree n on each interval [k, k+1) with $k \in Z$ when n is odd, and [k-1/2,k+1)] with $k \in Z$ when n is even. An equivalent definition of $S_n(IR)$, which is due to Schoenberg, states that any polynomial spline can be represented by a weighted sum of shifted B-splines and is therefore uniquely characterized by its sequence of B-spline coefficients c(k). The fundamental characteristic of the B-spline basis functions is their compact support. It is also possible to construct alternative sets of shift invariant basis functions $\{\varphi(x-k), k\in Z\}$ by taking linear combinations of B-splines [3]. In practice, it is often of interest to determine the B-spline coefficients of a polynomial spline fn(x) that precisely interpolates a given sequence of data points $\{f(k)\}k\in Z$ (discrete signal): this is the cardinal spline interpolation which can be obtained by digital filtering [2]. In summary, Unser-AlDroubi (resp. Shannon) theorem proceeds from the L_2 function, projects it into the spline (resp. band-limited) space with a continuous filtering, then sample the function into the spline (resp. band-limited) space and are capable of reconstructing the exact continuous version of it using a second continuous-discrete convolution equation which performs the interpolation step inside the given space.

3. DIRAC MOJETTE TRANSFORM

As judicious way to obtain a discrete exact Radon operator proceeds as follows. The continuous Radon transform described by :

$$proj(t,\theta)=\boldsymbol{R}\, f(x,y)= \int_{-\infty}^{+\infty}\int_{-\infty}^{+\infty} f(x,y)\, \delta(t -x\cos\theta +y\sin\theta)\, dxdy, \quad (1)$$

represents the continuous function f(x,y) by an infinite set of projections. The functional projection of f(x,y) onto a spline space $\{\varphi(x-k), k\in Z\}$ leads to an interpolation equation :

$$f\varphi\,(x,y) = \sum_{k=-\infty}^{+\infty}\sum_{l=-\infty}^{+\infty} f\,(k,l).\varphi(x-k).\varphi(y-l). \quad (2)$$

When the discrete pixel grid is considered in the tomographic problem, the function f(x,y) in Eq. (1) is replaced by $f\varphi\,(x,y)$ of Eq. (2). This leads (after inverting discrete and continuous sum signs) to a definition of the continuous projection from a discrete image and the spline interpolating function.
In this paragraph, φ is taken as $\varphi(x) = \delta(x)$. Eq. (1) becomes

$$proj_{\delta}(t,\theta) = \sum_{k=-\infty}^{+\infty}\sum_{l=-\infty}^{+\infty} f(k,l).\left[\int_{-\infty}^{+\infty}\int_{-\infty}^{+\infty}\delta(x-k)\delta(y-l)\delta(t-x\cos\theta+y\sin\theta)dxdy\right], \quad (3)$$

which simply reduces to:

$$proj_{\delta}(t,\theta)= \sum_{k=-\infty}^{+\infty} \sum_{l=-\infty}^{+\infty} f(k,l)\, \delta(t - k.\cos\theta + l.\sin\theta). \quad (4)$$

Since functions cosθ and sinθ are giving pure real values, (kcosθ +lsinθ) is of elliptical form and the only possibility to equally sample variable t is to use angles of the form $\tan\theta = \frac{q}{p}$. In such a case, $\cos\theta = \frac{p}{h}$ and $\sin\theta = \frac{q}{h}$, and Eq. (4) resumes as :

$$proj_{\delta}(t,p,q) = \sum_{k=-\infty}^{+\infty} \sum_{l=-\infty}^{+\infty} f(k,l)\ \delta(t.h - k.p + l.q) \quad (5)$$

To avoid ambiguities, only integer couples (p,q) with GCD(p,q) = 1 give acceptable angles; moreover, the q value is restricted to positive values. Performing the projection bin sampling leads to the Dirac-Mojette transform definition :

$$\mathbf{M}_{\delta}f(k,l)=proj(b,p,q)= \sum_{k=-\infty}^{+\infty} \sum_{l=-\infty}^{+\infty} f(k,l)\Delta(b-k.p+l.q) \quad (6)$$

where

$\Delta(b) = \begin{cases} 1 \text{ if } b=0 \\ 0 \text{ if } b \neq 0 \end{cases}$ is the discrete Kronecker symbol.

Notice that the discrete Mojette operator features some interesting properties as a variable number of bins onto a projection and an angle-dependant sample spacing. The direct and inverse algorithms exhibit a similar order of complexity of O(IN) where I is the number of projections and N the number of pixels. More theoretical results for inverse Mojette transform conditions are available on [4,5,6].

4. SPLINE MOJETTE TRANSFORM

4.1 Spline 0 Mojette transform definition

Let start with the Mojette transform for spline of zero order. In this case, the interpolator can be defined as :

$$\varphi_0(x) = \begin{cases} 1 \text{ si } |x| < ½ \\ ½ \text{ si } |x| = ½ \\ 0 \text{ sinon} \end{cases}. \quad (7)$$

In this case, Eq. (1) becomes

$$proj_0(t,\theta)= \sum_{k=-\infty}^{+\infty} \sum_{l=-\infty}^{+\infty} f(k,l).\ kernel_0(k,l,t,\theta) \quad (8)$$

$$\text{with } kernel_0(k,l,t,\theta) = \int_{-\infty}^{+\infty}\int_{-\infty}^{+\infty} \varphi_0(x-k)\ \varphi_0(y-l)\delta(t-\cos\theta+y)dxdy.$$

Using the same angle discretization as above leads to :

$$kernel_0(k,l,t,p,q)= \int_{-\infty}^{+\infty}\int_{-\infty}^{+\infty} \varphi_0(x-k)\ \varphi_0(y-l)\delta(th-px+qy)dxdy. \quad (9)$$

This transform projects each flat pixel and generates trapezoidal shapes onto the projection as depicted in figure 1. Next, the projection is sampled at rate b=th leading to the definition of the spline 0 Mojette transform :

$$\mathbf{M}_0 f(k,l)= \sum_{k=-\infty}^{+\infty} \sum_{l=-\infty}^{+\infty} f(k,l)kernel_0(k,l,b,p,q)\Delta(b-k.p+l.q) \quad (10)$$

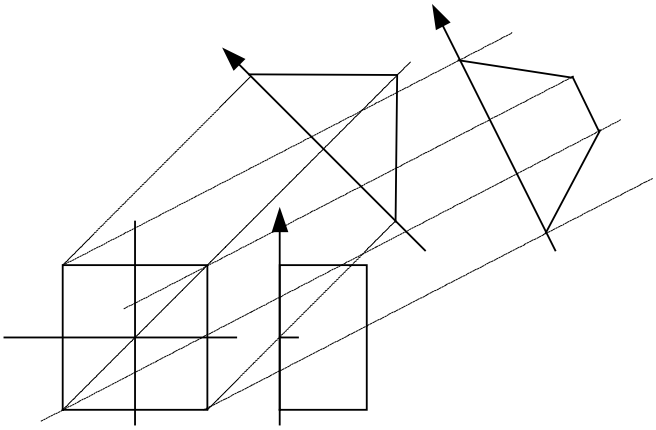

Figure 1 : Projections of a pixel for spline 0 Mojette.

Another way of expressing the spline-0 Mojette transform is to referred to the previous Dirac Mojette. Because of the particular sampling onto the projection, it it easy to see that the trapezoidal shape is always the result of the convolution of two step functions of integer width of p and q values.

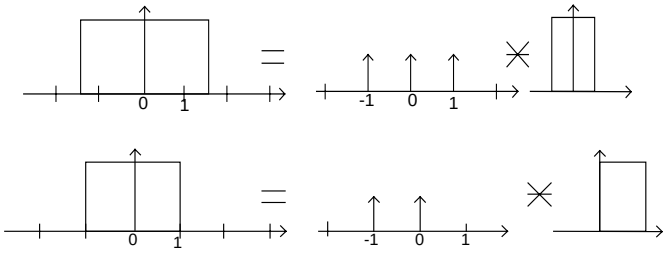

Figure 2 : Decomposition of integer width step functions.

The continuous expression of the convolution in (9) leads to different kernels $kernel_0(0,0,t,p,q)$ depending of the oddness of p and q (p and q can not be both even since GCD(p,q)=1). Figure 2 explains the way the trapezoidal shape is decomposed with respect to the 1D grid. This is summarized by Eqs (11) and (12) :

If p and q odd:

$$kernel_0(0,0,t,p,q)=\varphi_0(t)*\varphi_0(t)* \sum_{i=-\frac{p+1}{2}}^{\frac{p+1}{2}} \delta(t-i\Delta) * \sum_{j=-\frac{q+1}{2}}^{\frac{q+1}{2}} \delta(t-j\Delta) . \quad (11)$$

If p odd and q even :

$$kernel_0(0,0,t,p,q)=\varphi_0(t)*\varphi_0(t-\tfrac{1}{2})* \sum_{i=-\frac{q}{2}}^{\frac{q+1}{2}} \delta(t-i\Delta) * \sum_{j=-\frac{p+1}{2}}^{\frac{p+1}{2}} \delta(t-j\Delta) . \quad (12)$$

The goal is to obtain now a discrete version of the kernel to be used in Eq. (10). The sampling of the small Dirac combs is now easy and will not interfere with the sampling process. Since we have B-spline functions, $\varphi_1(x) = \varphi_0(x) * \varphi_0(x)$ which discrete version is only a centered Dirac, and $\varphi_0(t) * \varphi_0(t-\frac{1}{2})$ gives a small additional discrete kernel equals to (½ ½). Finally, the expression of the Spline 0 Mojette transform is given by :

$$\mathbf{M}_0 f(k,l) = \mathbf{M}_\delta f(k,l) * \text{kernel}_0(k,l,b,p,q), \quad (13)$$

with

$$\text{kernel}_0(0,0,b,p,q) = \begin{cases} \text{if p and q odd:} \\ \underbrace{(1\ 1\ 1\ \ldots\ 1)}_{p} * \underbrace{(1\ 1\ 1\ \ldots)}_{q} \\ \text{if p or q even:} \\ \tfrac{1}{2}\underbrace{(1\ 1\ 1\ \ldots\ 1)}_{p} * \underbrace{(1\ 1\ 1\ \ldots)}_{q} * (1\ 1) \end{cases} \quad (14)$$

The following table shows some examples of (p,q) angles decomposition :

(p,q)	Kernel	Decomposition
(1,0)	(1)	(1)
(1,1)	(1)	(1) *(1)
(2,1)	½ (1 2 1)	½(1 1)*(1 1) *(1)
(3,1)	(1 1 1)	(1 1 1) *(1)
(5,2)	½(1 3 4 4 3 1)	½(1 1)*(1 1 1 1 1) *(1 1)

Table 1 : Decomposition of some discrete kernels.

4.2 Spline n Mojette transform definition

Using B-spline basis allows for an easy generalization to higher spline order. From spline of order 0 to spline of order 1, only an additional convolution by the same discrete kernel has to be realized. Its definition is thus given by :

$$\mathbf{M}_1 f(k,l) = \mathbf{M}_0 f(k,l) * \text{kernel}_0(k,l,b,p,q), \quad (15)$$

Definition of the spline of order n Mojette transform only needs to performs the (n+1) convolutions by $\text{kernel}_0(k,l,b,p,q)$ from the projections obtained by Eq. (6).

It is important here to precise that the obtained projections (or image) are not interpolative splines but only coefficients. However, the use of B-spline in this context is relevant since the smoothing effect (correlation onto the projections) will be the key for stable communications in the applications. If one desires the image or projection obtained from the B-spline coefficients this is also obtained by discrete convolutions [1].

4.3 Spline n Mojette algorithms

Algorithms to compute the direct transform of the spline-n Mojette transform directly follow from Eqs. (6),(13), and (15). For a single projection (p,q), Eq. (6) computes the initial projection in O(N) where N is the number of pixels. Then the small convolutions by "1" kernels can start. Notice that such a convolution can be performed by shifting the projection line and adding the original and shifted lines. Inverting Eq. (6) has been presented in [4,5]. Inverting Eq. (13) can be simply made by a recursive filtering which is also very simple to implement here thanks to the very simple filters derived in Eq. (14).

5. APPLICATIONS

5.1 Tomography

The Dirac-Mojette transform is a very interesting tool for image processing since it only uses additions (resp. subtractions) to compute the direct (resp. inverse) transform. However, this version can not be useful for tomographic reconstruction since only "discrete" lines are summed up. However, the spline 0 Mojette transform corresponds to a summation of the entire Euclidean line as shown in Fig. 3 which compares the Dirac and spline 0 Mojette projection at angle (2,1).

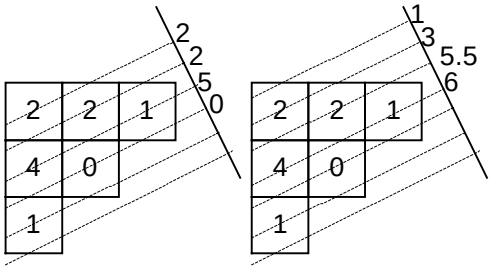

Figure 3 : Projections of an image corner at angle (2,1).

Tomographic devices are nowadays enough accurate to simulate the angle demanded by the angular specificities of the Mojette transform. However, the sampling onto the projection is variable and very fine which can not be directly implemented. In the case of parallel acquisitions systems the use of other spline approximations (noise regularization onto the projection prior to reconstruction) are on study to solve for it. In the case of non-parallel acquisition (e.g. X-ray scanner or PET) each bin value can be approximated first with respect to the discrete acquisition geometry. Then a second step is to use the spline Mojette transform in a random variable context to perform the reconstruction. In that case, the major advance is the exact treatment of the null space of the discrete inverse operator which is connected to the discrete tomography field (polyaminos). Instead of using the continuous theory which decomposes the null space with Bessel functions and does not take into account the discrete number of counts per bin, the inverse spline Mojette operator provides a decomposition of its null space in terms of "phantoms" corresponding to convolutions of valuated two pixels elements in the directions of projections.

5.2 Error correcting codes for information transmissions

The multiple information description is of great interest for packet communications. By spreading the initial information into two (or more) bulks of information with redundancy between each portion, it allows for packet losses onto the network. The Dirac Mojette transform has proven its adequacy to solve for this problem. The initial information (generally a bitstream) is first mapped onto a "2D geometrical buffer" which is projected onto a set of redundant projections (the redundancy is chosen according to network losses statistics). The possibility of reconstructing the initial data from a set of (I-L) packets when I projections (packets) are computed and sent and L packets are lost can be easily built with the Mojette transform. Notice that for network communications, the summation operator is replaced with a XOR. The first interest

of the Mojette transform is to generalize the number of descriptions that can be used. The second advantage is to use a scalable description of the source (e.g. available for JPEG2000, SPIHT, MPEG4 CoDecs) and to transmit these projections (using a specific kind of geometrical buffer) along a network which does not implement quality of service properties as the Internet Protocol.
However, the Dirac Mojette transform does not take into account the possible noise degradations of the sent packets. More and more network protocols tends to lighten their correcting codes for efficient data transmission because of the real-time constraints. If packets are going through mobile communications the ratio of noisy packets at destination will seriously increase. The spline Mojette transform is a good candidate for taking care of that problem. After the multiple description onto a geometrical buffer has been computed with the Dirac Mojette transform, data can be correlated by using the spline Mojette transform according to Eqs. (13,15). Each spline projection is then taller than the Dirac projection with a number of additional bins corresponding to the kernel described in Eq. (14). This can be viewed as an error correcting code onto each projection (whereas the Mojette transform by itself realizes a distributed error correcting code which power seems to corresponds to the number of projections minus one). Of course, the higher the noise encountered in the network, the higher spline order. Therefore, the spline order can be tune according to communications properties in real time if a feedback signaling channel is implemented (e.g. RTP for the Internet protocol). The last point to derive in this context is to understand the collaboration between the two error correcting codes implemented with the spline Mojette transform.

6. CONCLUSION

In this paper, the extension to the spline Mojette transform was presented. The discrete character of the transform allows for fast implementations. As for the classical spline theory, going from a spline order to another can always be made by small convolutions. The Dirac Mojette transform which has been used for five years for communications and image processing can be gracefully extended to the spline Mojette transform thanks to small additional kernels. Recursive filtering can be used to recover the Dirac Mojette transform from the spline Mojette transform. This allows for an optimal (linear) complexity in decoding the projections set. The spline Mojette transform is imperative to implement for new tomographic devices since the Dirac Mojette transform can not accurately represents the physical projection process. In packet communications, the role of the spline Mojette transform is to fight against noise via the additional smoothing provided by the B-spline coefficients that are transmitted (instead of the original samples). This efficient coding is able to react to the network real-time constraints both for losses and noise degradations.

7. REFERENCES

[1] M. Unser, A. AlDroubi, M. Eden, “Polynomial spline signal approximations: filter design and asymptotic equivalence with Shannon’s sampling theorem”, IEEE Trans. Information Theory, vol. 38, pp. 95-103, January 1992.

[2] A. AlDroubi , M. Unser, "Families of wavelet transforms in connection with Shannon sampling theory and the Gabor transform” in Wavelets – A tutorial in theory and applications, CK. Chui, Ed., San Diego: Academic Press, pp. 509-528, 1992.

[3] M. Unser, A. AlDroubi, M. Eden,
"B-spline signal processing. Part 1: theory”, IEEE Trans. Signal Processing, vol 41, February 1993.
"B-spline signal processing. Part 2: efficient design and applications”, IEEE Trans. Signal Processing, vol 41, February 1993.

[4] N. Normand, JP. Guédon, "The Mojette transform : a redundant transformation for image representation” Comptes-Rendus de l’Académie des Sciences de Paris. Section theoretical computer science, pp.123-126, January 1998.

[5] O. Philippé, JP. Guédon, "Correlation properties of the Mojette representation for non-exact image reconstruction," Proc. Picture Coding Symposium 97, Berlin, ITG-Fachbericht Verlag Ed., pp. 237-241. September 1997.

[6] JP. Guédon, B. Parrein, N. Normand, "Internet distributed image information system” , Integrated Computer-Aided Engineering, vol. 8, p. 205-214, August 2001.